PHYSICAL REVIEW B **72**, 241305(R) (2005)

Internal electric field in wurtzite $ZnO/Zn_{0.78}Mg_{0.22}O$ quantum wells

C. Morhain,[1] T. Bretagnon,[2] P. Lefebvre,[2,*] X. Tang,[1] P. Valvin,[2] T. Guillet,[2] B. Gil,[2] T. Taliercio,[2] M. Teisseire-Doninelli,[1] B. Vinter,[1] and C. Deparis[1]

[1]*Centre de Recherche sur l'Hétéro-Epitaxie et ses Applications—CNRS, Rue Bernard Grégory, F-06560 Valbonne, France*

[2]*Groupe d'Etude des Semiconducteurs—CNRS—Université Montpellier II, Case Courrier 074, F-34095 Montpellier Cedex 5, France*

(Received 5 October 2005; revised manuscript received 10 November 2005; published 12 December 2005)

Continuous-wave, time-integrated, and time-resolved photoluminescence experiments are used to study the excitonic optical recombinations in wurtzite $ZnO/Zn_{0.78}Mg_{0.22}O$ quantum wells of varying widths. By comparing experimental results with a variational calculation of excitonic energies and oscillator strengths, we determine the magnitude (0.9 MV/cm) of the longitudinal electric field that is induced by both spontaneous and piezoelectric polarizations. The quantum-confined Stark effect counteracts quantum confinement effects for well widths larger than 3 nm, leading to emission energies that can lie 0.5 eV *below* the ZnO excitonic gap and to radiative lifetimes that can be larger than milliseconds.

DOI: 10.1103/PhysRevB.72.241305 PACS number(s): 78.67.De, 78.66.Hf, 78.47.+p, 73.21.Fg

For the past 20 years, increasing complexity has been introduced in the modeling and in the manipulation of quantum states in semiconductor nanostructures such as quantum wells (QWs) or quantum dots. To control the energies and wave functions of electrons and holes, and excitonic optical transitions, a number of physical interactions, intricately related to quantum confinement, have to be considered: internal strains, Coulomb interaction, coupling to polar phonons, possible built-in electric fields, etc. The relative importance and the size dependence of each of these effects is dependent on the properties of the given material system. III-V or II-VI compounds, narrow or wide band gap semiconductors, or cubic or hexagonal crystals produce a variety of physical behaviors, e.g., the presence of huge built-in electric fields.

Such fields were found to appear naturally in strained QWs based on zinc blende III-V or II-VI semiconductors, grown away from the (001) direction,[1] both in type I (Refs. 2 and 3) and in type II configurations.[4] For type I systems, where both electron and hole are confined in the same layer, the resulting quantum-confined Stark effect (QCSE) redshifts the fundamental optical transition but it also reduces the 1*s* exciton binding energy. It also reduces the exciton oscillator strength by separating the wave functions of the electron and hole and by loosening the Coulomb attraction that controls the extension of their in-plane relative motion. Giant effects of this nature have been observed in QWs based on wurtzite group-III nitrides which exhibit large coefficients of both spontaneous and piezoelectric polarizations (comparable to those of ZnO Refs. 5 and 6) and thus can generate internal fields of several MV/cm. For nitride QWs wider than a few nanometers, the QCSE is so strong that it counteracts the quantum confinement and therefore pushes the fundamental transition below the excitonic gap of the QW material. Two regimes can be defined: (i) For narrow QWs, the quantum confinement dominates, yielding large emission energies and typical excitonic lifetimes of nanoseconds, or slightly less. (ii) For sufficiently wide QWs, the QCSE dominates and the emission energy decreases almost linearly with increasing L_W, whereas the exciton lifetime increases (its oscillator strength decreases) almost exponentially.[7]

In principle, ZnO-based quantum structures are expected to present similar effects, owing to the wurtzite crystal structure of this compound and to particularly large coefficients for both piezoelectric and spontaneous polarizations. This specificity of ZnO opens different perspectives since quantum nanostructures, such as ZnO/(Zn,Mg)O QWs, are now becoming available. To model the optical properties of such systems, competitive effects of confinement and electric fields on the presumably large exciton binding energy (~60 meV for bulk ZnO, see Ref. 8), will have to be properly considered. To date, no quantitative data are available concerning the polarization properties of (Zn,Mg)O or MgO in their wurtzite phase. Nevertheless, ZnO/(Zn,Mg)O QWs have recently been produced and their physical properties have been studied in a number of experimental papers.[9–22] In fact, very few of these papers[14–16] qualitatively evoke the presence of an internal electric field. Theoretically, all available calculations of interband transitions[9,17–19,23] or excitonic properties[13,23] have ignored, to date, this possibility, although it was predicted by symmetry arguments. Reference to "piezoelectric confinement" at $ZnO/Zn_{0.6}Mg_{0.4}O$ interface was recently made.[24]

In this paper, we report results of continuous-wave (cw), time-integrated and time-resolved (TR) photoluminescence (PL) experiments performed on a series of wurtzite $ZnO/Zn_{0.78}Mg_{0.22}O$ QW samples. We demonstrate the presence of a large electric field along the (0001) growth direction. We estimate the magnitude of this field by an envelope-function model that includes the variational calculation of the exciton binding energy. This model accounts very well for the well width dependence of both the PL energy and decay time.

Samples containing one or two QWs were grown by molecular beam epitaxy on the *c* plane of sapphire substrates, following the deposition of 1-μm-thick ZnO templates. The residual electron density in the QW area is estimated to be less than 10^{16} cm^{-3}. Details on the growth process will be given elsewhere,[25] but it is worthwhile mentioning that the width, L_B, of the $Zn_{0.78}Mg_{0.22}O$ barriers is quite large (200 nm). This ensures that the electric field, if any, in the QWs assumes its maximum possible value. Indeed, for mul-

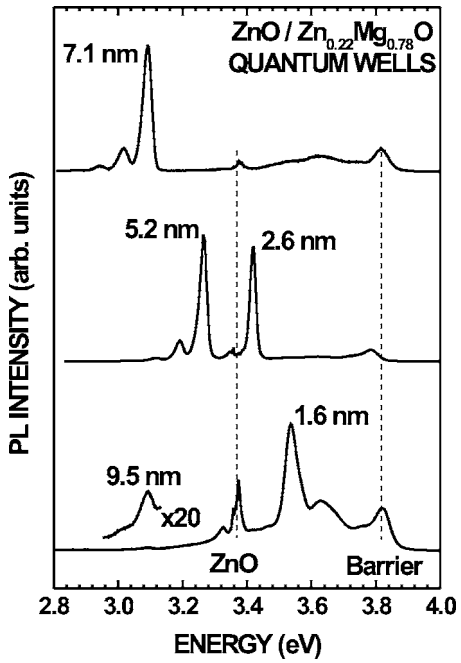

FIG. 1. Continuous-wave PL spectra of $ZnO/Zn_{0.78}Mg_{0.22}O$ QWs of various widths, as indicated, taken at $T=10$ K. The pump-power density was 100 mW/cm^2. The PL energies from the $Zn_{0.78}Mg_{0.22}O$ barrier layers and those of the ZnO buffer layers are shown by dashed lines.

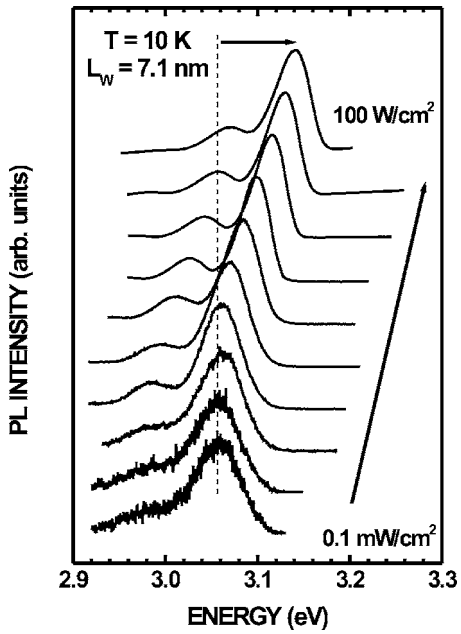

FIG. 2. Continuous-wave PL spectra of the 7.1-nm QW, for various pump-power densities. The highest power density (top spectrum) is 100 W/cm^2. This density was divided by a factor 3.1 and again for the six higher energy spectra. Then, between the four lower energy spectra a factor of 10 was applied.

tiple QWs with well width L_W, the field in the well is known[26] to be approximately proportional to the "geometrical factor" $L_B/(L_W+L_B)$. This effect explains, to a large extent, why previous works, reporting on narrow-barrier multiple QWs, did not mention any sizable electric fields. The second reason why previous works were not conclusive on this issue is that most of the samples lay in the first regime described above: the QCSE was not the dominant effect because the well width seldom exceeded 4 nm. Our samples cover a wide range of well widths (L_W=1.6, 2.6, 5.2, 7.1, and 9.5 nm, respectively).

Figure 1 shows the cw PL spectra, recorded at 10 K, of the various investigated samples, whereas the excitation was provided by the 244-nm line of a frequency-doubled argon ion laser. The first direct evidence of the presence of a strong electric field is given by the PL lines of the three wider QWs, which all lie below the ZnO excitonic gap. The strength of coupling of excitons to LO-phonons appears to be a growing function of L_W, as shown by the growing relative intensities of phonon replicas. This is another effect of the electric field.[27]

Further evidence for the presence of large built-in electric fields in the QWs is provided by the pump-power dependence of their emission energy. While this effect remains small in the narrower QWs, it can be very large in the wider ones, as shown in Fig. 2, where a blueshift of ~80 meV is observed by increasing the pump-power density from 0.1 up to 100 W/cm^2. This results from the screening of the internal electric field by high densities of electron-hole dipoles. Such effects can be produced at moderate excitation densities because of the large recombination time that we establish below, for the wider QWs. Nevertheless, the power densities available on our setup were not large enough to permit the full screening of the internal field. Such a screening would yield PL energies above the ZnO excitonic gap and thus would permit a direct estimation of the QCSE. However, a prerequisite for this is the knowledge of the minimum PL energy that the system can reach. For the lower energy PL spectrum in Fig. 2, for instance, we realized that the internal field was in fact slightly screened, as shown below. We thus needed to quantify as precisely as possible the values of PL energies and recombination times that correspond to the situation of unscreened electric fields. For this purpose, we have performed careful time-integrated and time-resolved PL measurements.

Indeed, in the following, we use results of time-integrated PL, obtained under pulsed excitation, instead of cw PL. The 2-ps laser pulses were provided by the third harmonic ($\lambda \sim 260$ nm) of a titanium-sapphire laser, with typical energy densities of ~50 nJ/cm^2 per pulse. The repetition rate was adapted to the slowness of the observed decay, by use of an acousto-optical modulator, between 800 Hz and 80 kHz, thus allowing for a full de-excitation between two consecutive pulses. The only exception is for our widest QW (L_W=9.5 nm), for which we have used 5-ns pulses of the fourth harmonic (266 nm) of a yttrium aluminum garnet (YAG):Nd laser, with a repetition rate of 10 Hz, with typical energy density of 500 μJ/cm^2 per pulse. For the widest QWs, the temporary screening[4,28] of the internal electric field by large densities of *e-h* pairs induced some time dependence of the PL energy in the first few tens or hundreds of nanoseconds after excitation. In such cases, to obtain the "real" PL energies plotted in Fig. 3, we have restricted the

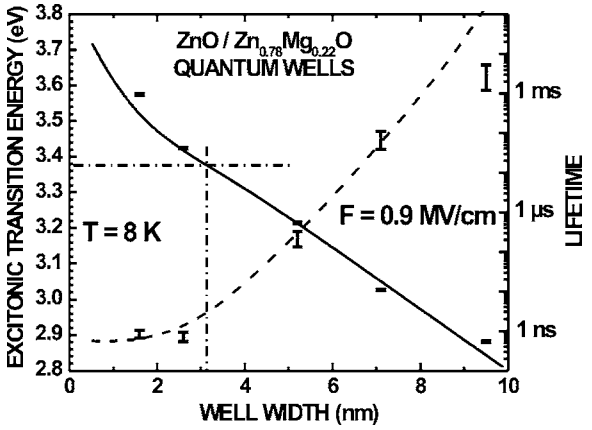

FIG. 3. Horizontal segments show the PL peak energies, compared to the result of our variational calculation (solid curve). The dash-dotted lines show the excitonic gap of ZnO and the critical well width separating the two regimes of confinement (see text). A dashed curve shows the well width dependence of term f, multiplied by a factor of 7×10^{-4} in order to be compared with the experimental PL decay times, shown with error bars.

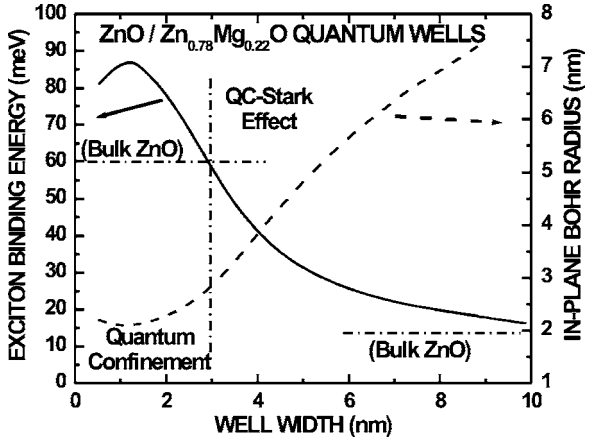

FIG. 4. Calculated binding energy (left) and pseudo-Bohr radius (right) vs well width, obtained by assuming an electric field of 0.9 MV/cm.

time-integration window to delays large enough to ensure the constancy of the emission energy. It is worth mentioning, here, that cw PL provides emission energies that can be higher by several tens of meV than those shown in Fig. 3, especially for the three wider QWs (see Fig. 1).

To account for our experimental results, we have calculated the recombination energy, the binding energy, and the oscillator strength of the ground-state exciton by a variational model[29] that includes the electric field. We have used a set of numerical parameters that is consistent with previous works:[9,23,30,31] $m_e=0.24$ and $m_h=0.78$ for electron and hole on-axis effective masses in both well and barrier materials, $\varepsilon_b=6.4$ for the background dielectric constant,[8] consistently with an exciton binding energy of 60 meV. We measured a band-gap difference of 0.47 eV between $Zn_{0.78}Mg_{0.22}O$ and ZnO, from our PL experiments, and we chose a conduction band offset ratio of 0.8. We describe the exciton relative motion by the product of envelope functions $f_e(z_e)$ and $f_h(z_h)$ accounting for the electron and hole confinement along the growth axis, by the two-dimensional hydrogenic term $\varphi_\lambda(\rho)=(\sqrt{2/\pi}/\lambda)\exp(-\rho/\lambda)$, where ρ is the in-plane relative coordinate. The variational parameter, λ, is the in-plane pseudo-Bohr radius that is varied in order to minimize the overall energy of the Coulomb-correlated electron-hole pair. Our calculation shows a very good agreement with experimental PL energies (Fig. 3), when we include an electric field of 0.9 MV/cm. It is important to note that the fitting electric field value really depends on the variation of the exciton binding energy. By ignoring this variation, the fitting value becomes 0.8 MV/cm. As a matter of fact (Fig. 4), the binding energy decreases by nearly 70 meV when L_W varies from 1.6 to 9.5 nm. For narrow QWs, the confinement enhances the exciton binding energy, as discussed in previous experimental and theoretical works.[13,23] But this energy becomes smaller than its bulk value, for $L_W>3$ nm. Contrary to recent calculations,[23] we find that the binding energy can be smaller than 20 meV for $L_W>9$ nm, because we account for the electric field. As pointed out by Coli and Bajaj,[23] the coupling of excitons to phonons certainly affects their binding energies, for such polar compounds. But this effect should be included in the context of large electric fields.

Our calculation of the Coulomb term is valid for free excitons or for excitons that are localized, as a whole, on areas having in-plane dimensions much larger than the in-plane Bohr radius. If the localization radius of the electron or the hole is smaller than, say, 7 nm (see Fig. 4)—which we do not know—the binding energy might be slightly larger than the one shown in Fig. 4, for the wider QWs. For the latter, due to the electric field, electrons and holes might be independently localized, which differs from the case of localized, "rigid" excitons.[32] This affects more the recombination dynamics than the L_W dependence of the Coulomb correlation energy of electron-hole pairs that have strong recombination probability.

Figure 3 also shows the measured PL decay times. We must mention that, for all QWs that emit below the ZnO band gap, the measured PL decays could be well fitted by single-exponential functions. On the other hand, the decays for the two narrower QWs were more complex. In Fig. 3, we only present the fast decay time that we extract by fitting the beginning of the PL decay over one order of magnitude. This dynamics is followed by a slower one, which we are currently studying. These results are compared (dashed line) to the corresponding well width dependence of the quantity $f=|\varphi_\lambda(0)|^{-2}|\int_{-\infty}^{+\infty}dz f_e(z)f_h(z)|^{-2}$, which is, in this "one band" approximation, proportional to the exciton radiative lifetime. We have simply multiplied f by a unique coefficient in order to fit the measured PL decay times for the four narrower wells. The calculated lifetime increases by more than 8 orders of magnitude between $L_W=2$ and 9 nm. For our widest QW ($L_W=9.5$ nm), this calculation predicts a lifetime of $\sim$100 ms, i.e., much larger than the $\sim$3 ms that we measured. We explain this discrepancy by the residual screening of the internal electric field by accumulated e-h pairs.[4,28] This occurred, despite our experimental care, because our interpulse interval of 100 ms is still too small, compared to the predictable lifetime. This explanation is consistent with

the observation of a time-integrated PL energy lying a few tens of meV above the calculated one (see Fig. 3), for this QW.

In summary, we performed cw, time-integrated, and time-resolved PL spectroscopy on wurtzite $ZnO/Zn_{0.78}Mg_{0.22}O$ quantum wells grown along the (0001). By comparing experimental PL energies and the results of a variational, excitonic calculation, we determined the internal electric field in this system. We obtained 0.9 MV/cm, which leads, by linear interpolation to a maximum field of 4.1 x (in MV/cm), for $ZnO/Zn_{1-x}Mg_xO$ QWs. We also measured the well width dependence of PL decay times, over several orders of magnitude. This dependence is well accounted for by our calculation of excitonic oscillator strengths.

*Corresponding author.

[1] D. L. Smith and C. Mailhiot, J. Appl. Phys. **63**, 2717 (1988).
[2] P. Boring, B. Gil, and K. J. Moore, Phys. Rev. Lett. **71**, 1875 (1993).
[3] R. André, C. Deshayes, J. Cibert, Le Si Dang, S. Tatarenko, and K. Saminadayar, Phys. Rev. B **42**, 11392 (1990).
[4] W. Langbein, M. Hetterich, and C. Klingshirn, Phys. Rev. B **51**, 9922 (1995).
[5] F. Bernardini and V. Fiorentini, Phys. Rev. B **57**, R9427 (1998).
[6] Y. Noel, C. M. Zicovich-Wilson, B. Civalleri, Ph. D'Arco, and R. Dovesi, Phys. Rev. B **65**, 014111 (2001).
[7] See, e.g., P. Lefebvre, A. Morel, M. Gallart, T. Taliercio, J. Allègre, B. Gil, H. Mathieu, B. Damilano, N. Grandjean, and J. Massies, Appl. Phys. Lett. **78**, 1252 (2001), and references cited therein.
[8] N. N. Syrbu, I. M. Tiginyanu, V. V. Salamai, V. V. Ursaki, and E. V. Rusu, Physica B **353**, 111 (2004).
[9] T. Makino, C. H. Chia, Nguen T. Tuan, H. D. Sun, Y. Segawa, M. Kawasaki, A. Ohtomo, K. Tamura, and H. Koinuma, Appl. Phys. Lett. **77**, 975 (2000).
[10] H. D. Sun, T. Makino, N. T. Tuan, Y. Segawa, Z. K. Tang, G. K. L. Wong, M. Kawasaki, A. Ohtomo, K. Tamura, and H. Koinuma, Appl. Phys. Lett. **77**, 4250 (2000).
[11] T. Makino, N. T. Tuan, H. D. Sun, C. H. Chia, Y. Segawa, M. Kawasaki, A. Ohtomo, K. Tamura, T. Suemoto, H. Akiyama, M. Baba, S. Saito, T. Tomita, and H. Koinuma, Appl. Phys. Lett. **78**, 1979 (2001).
[12] C. H. Chia, T. Makino, Y. Segawa, M. Kawasaki, A. Ohtomo, K. Tamura, and H. Koinuma, J. Appl. Phys. **90**, 3650 (2001).
[13] H. D. Sun, T. Makino, Y. Segawa, M. Kawasaki, A. Ohtomo, and H. Koinuma, J. Appl. Phys. **91**, 1993 (2002).
[14] T. Makino, K. Tamura, C. H. Chia, Y. Segawa, M. Kawasaki, A. Ohtomo, and H. Koinuma, Phys. Rev. B **66**, 233305 (2002).
[15] T. Makino, K. Tamura, C. H. Chia, Y. Segawa, M. Kawasaki, A. Ohtomo, and H. Koinuma, Appl. Phys. Lett. **81**, 2355 (2002).
[16] T. Makino, A. Ohtomo, C. H. Chia, Y. Segawa, H. Koinuma, and M. Kawasaki, Physica E (Amsterdam) **21**, 671 (2004).
[17] S. Krishnamoorthy, A. A. Iliadis, A. Inumpudi, S. Choopun, R. D. Vispute, and T. Venkatesan, Solid-State Electron. **46**, 1633 (2002).
[18] Th. Gruber, C. Kirchner, R. Kling, F. Reuss, and A. Waag, Appl. Phys. Lett. **84**, 5359 (2004).
[19] B. P. Zhang, N. T. Binh, K. Wakatsuki, C. Y. Liu, Y. Segawa, and N. Usami, Appl. Phys. Lett. **86**, 032105 (2005).
[20] T. Yatsui, J. Lim, M. Ohtsu, S. J. An, and G.-C. Yi, Appl. Phys. Lett. **85**, 727 (2004).
[21] Won Il Park, Sung Jin An, Jia Long Yang, Gyu-Chul Yi, Sangsu Hong, Taiha Joo, and Miyoung Kim, J. Phys. Chem. B **108**, 15457 (2004).
[22] S. Sadofev, S. Blumstengel, J. Cui, J. Puls, S. Rogaschewski, P. Schäfer, Yu. G. Sadofyev, and F. Henneberger, Appl. Phys. Lett. **87**, 091903 (2005).
[23] G. Coli and K. K. Bajaj, Appl. Phys. Lett. **78**, 2861 (2001).
[24] K. Koike, K. Hama, I. Nakashima, G. Takada, M. Ozaki, K. Ogata, S. Sasa, M. Inoue, and M. Yano, Jpn. J. Appl. Phys., Part 2 **43**, L1372 (2004).
[25] C. Morhain *et al.* (unpublished).
[26] M. Leroux, N. Grandjean, J. Massies, B. Gil, P. Lefebvre, and P. Bigenwald, Phys. Rev. B **60**, 1496 (1999), and references cited therein.
[27] S. Kalliakos, X. B. Zhang, T. Taliercio, P. Lefebvre, B. Gil, N. Grandjean, B. Damilano, and J. Massies, Appl. Phys. Lett. **80**, 428 (2002).
[28] P. Lefebvre, S. Kalliakos, T. Bretagnon, P. Valvin, T. Taliercio, B. Gil, N. Grandjean, and J. Massies, Phys. Rev. B **69**, 035307 (2004).
[29] P. Bigenwald, P. Lefebvre, T. Bretagnon, and B. Gil, Phys. Status Solidi B **216**, 371 (1999).
[30] B. Gil, A. Lusson, V. Sallet, S. A. Said-Hassani, R. Triboulet, and P. Bigenwald, Jpn. J. Appl. Phys., Part 2 **40**, L1089 (2001).
[31] B. Gil, Phys. Rev. B **64**, 201310(R) (2001). Please note the inversion of labeling of *A* and *C* states in Fig. 2 of this reference.
[32] A. Morel, P. Lefebvre, S. Kalliakos, T. Taliercio, T. Bretagnon, and B. Gil, Phys. Rev. B **68**, 045331 (2003).